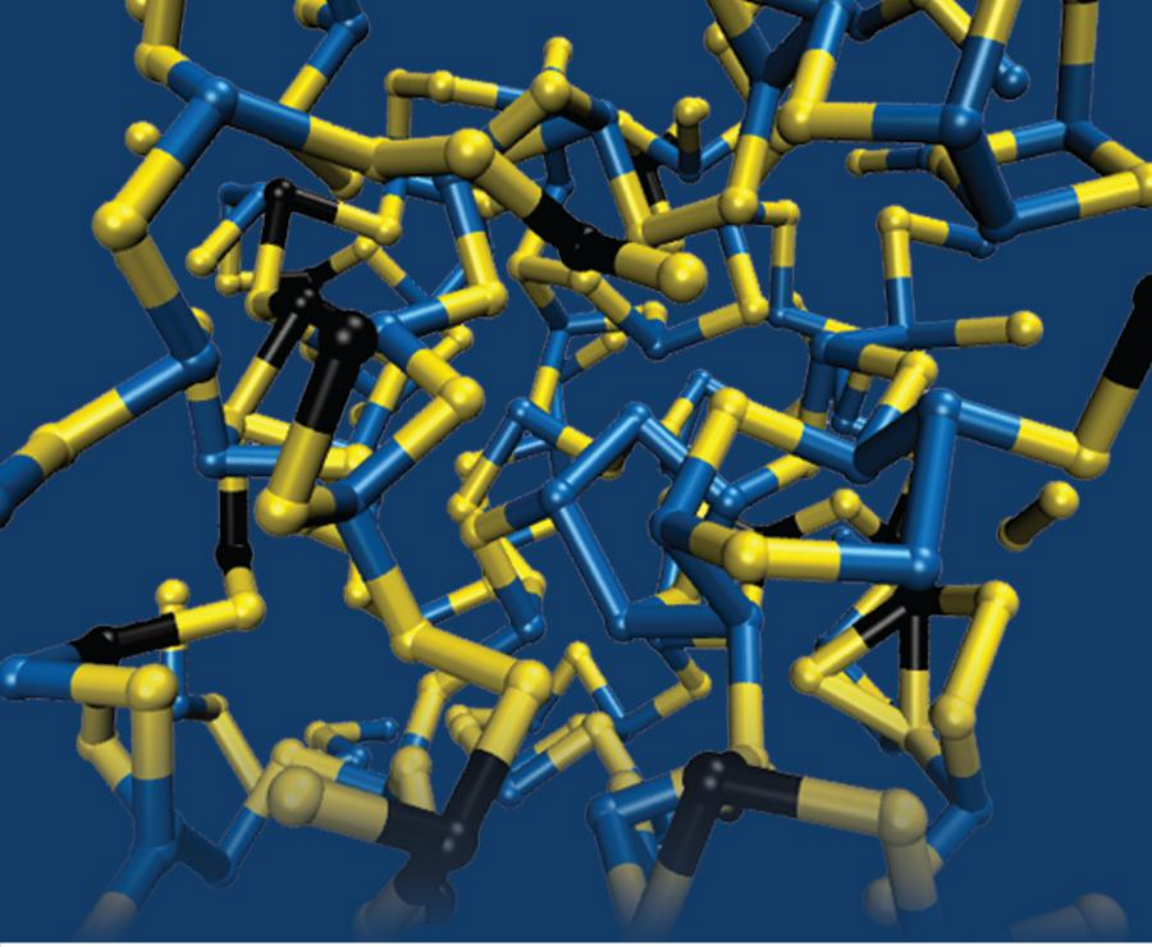

edited by

**Rongping Wang**

# AMORPHOUS CHALCOGENIDES

## Advances and Applications

# AMORPHOUS CHALCOGENIDES

This page intentionally left blank

edited by
**Rongping Wang**

# AMORPHOUS CHALCOGENIDES

## Advances and Applications

PAN STANFORD PUBLISHING

CRC Press
Taylor & Francis Group
6000 Broken Sound Parkway NW, Suite 300
Boca Raton, FL 33487-2742


Version Date: 20140213

International Standard Book Number-13: 978-981-4411-30-1 (eBook - PDF)

# Contents

# Preface

The research on the fundamental physics and practical applications of chalcogenide glasses has rapidly grown recently. This is mostly stimulated by commercially successful products based on glasses, such as xerographic photoreceptors in copying machines and digital versatile disks.

This book reviews the recent progress in the physics and applications of chalcogenide glasses. It begins with a discussion on the problem of glass formation in chalcogenide systems and then moves onto relaxation and fragility, as well as photoinduced deformation in glasses, experimental investigations, and computer simulation of the glass structure, followed by various applications such as optical amplifiers, sensors, and waveguide devices. The contributors to the book are experts in their fields. Therefore, although the book does not cover all the aspects of chalcogenide glasses, it certainly helps readers understand the fundamental concepts and the essence of the subject.

This book can be used by researchers and postgraduate students as a starting point to get familiar with the history/background and current status of the research topics discussed in the book.

I am grateful to all the chapter contributors. This book would not have been possible without their commitment and cooperation. I am grateful to the managing editor and the entire team at Pan Stanford Publishing for their assistance. Last, but not least, I thank my wife, Chunjiao, and my kids, Evanthy and Kevin, for their understanding and support while I spent a lot of family time on the book.

**Rongping Wang**

This page intentionally left blank

# Chapter 1

# Glass Formation in Several Novel Chalcogenide Systems

**Guorong Chen**
*School of Materials Science and Engineering,*
*East China University of Science and Technology,*
*Shanghai 200237, China*
grchen@ecust.edu.cn

As an important class of noncrystalline solids with a broad range of possible glass-forming systems and a large composition space, including nonstoichiometry possibility, chalcogenide (ChG) glasses have unique infrared-transmitting and infrared-semiconducting properties for practical applications in both military and civil fields [1] To extend transparency into the visible region, alkali halides have been introduced into the ChG system, producing the so-called chalcohalide (ChH) glasses. As halogen atoms from halides play a key role in ChH glasses by fixing the lone pair of electrons on the chalcogen atom (S, Se, Te), affording a considerably increased electronic bandgap [2], ChH glasses become more transparent in the visible region. This chapter focuses on recent work by our group on glass formation in some new ChG/ChH systems.

*Amorphous Chalcogenides: Advances and Applications*
Edited by Rongping Wang

ISBN 978-981-4411-29-5 (Hardcover), 978-981-4411-30-1 (eBook)
www.panstanford.com

## 1.1 The $GeS_2$–$Sb_2S_3$–PbS System

A large glass-forming region is found in the novel $GeS_2$–$Sb_2S_3$–PbS system with the incorporation of PbS up to 58 at.% [3]. Infrared (IR)-transmitting glass ceramics with a large amount of small-sized crystals (~100 nm) are produced by choosing substable compositions and annealing at fairly low temperatures (15–30°C above $T_g$, glass transition temperature) for longer durations (up to 100 hr). Crystals are identified by X-ray diffraction (XRD) as $Pb_2GeS_4$, $PbGeS_3$, PbS, or $PbSb_2S_4$, depending on base glass compositions. Compared with base glasses, glass ceramics shows a lower thermal expansion coefficient and higher fracture toughness, making them good candidate materials for IR optics.

### 1.1.1 Glass-Forming Region

The glass-forming region in the $GeS_2$–$Sb_2S_3$–PbS system was determined using 45 compositions by the conventional melt-quenching method. The weighed batches (10 g) were sealed into cleaned quartz glass ampoules under a vacuum of $10^{-3}$ Pa and melted at 850–950°C for more than 10 hr in a rocking furnace. The bulk samples were obtained by quenching the melts in water. Figure 1.1 shows the glass-forming region of the $GeS_2$–$Sb_2S_3$–PbS system.

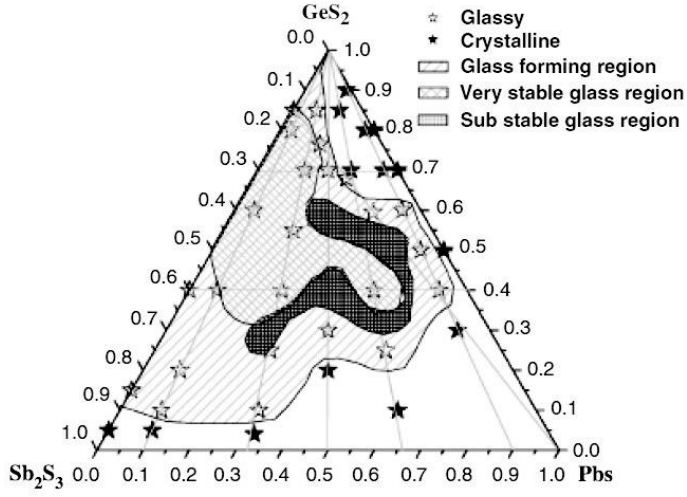


**Figure 1.1** Glass-forming region in the $GeS_2$–$Sb_2S_3$–PbS system (at.%).

Figure 1.1 shows that there is no glass formed in either the binary GeS–PbS or the $Sb_2S_3$–PbS system due to the poor glass-forming ability of single-component $GeS_2$ or $Sb_2S_3$. A fairly large glass-forming region is observed when PbS is incorporated into the binary $GeS_2$–$Sb_2S_3$ system, forming the ternary $GeS_2$–$Sb_2S_3$–PbS system, and the maximum PbS involvement is up to 58 at.%. This may be due to the competition of crystallization between these two units close to their eutectic point and thus increases the barrier for crystallization. Similar results have been reported on the $GeSe_2$–$As_2Se_3$–CdSe system, where introduction of $As_2Se_3$ improved the thermal stability of glasses [4].

### 1.1.2 Controlled Crystallization

Controlled crystallization of glass samples has been tried with typical annealing temperatures of 15–80°C above $T_g$ and characterized by scanning electron microscopy (SEM) (Fig. 1.2), XRD (Fig. 1.3), and visible and IR transmission spectra (Fig. 1.4).

It is observed that some glasses are not able to crystallize while being annealed at any temperatures between $T_g$ and $T_c$, even for a very long duration (>100 hr). A common characteristic of these glasses is a larger $\Delta T$ (>170°C, $T_c - T_g$) or even no exothermal peak in their differential scanning calorimetry (DSC) curves. We classify these compositions as very stable glasses (VSGs) in the glass-forming region (Fig. 1.1). For example, no crystals are observed after annealing sample G1 ($55GeS_2$–$30Sb_2S_3$–15PbS) at 330°C ($T_g$ + 55°C) for 163 hr, as shown in Fig. 1.2a.

Contrary to VSGs, glasses with compositions close to the border of the glass-forming region are too unstable to be controlled for crystallization. As it is very difficult to control the growth of crystals during annealing, crystals become too large in a short time, thus affecting IR transmission of materials. Moreover, the amount of crystals was too small to improve the physical and thermal properties of base glasses or even exert a negative effect. For example, few but large crystals are seen for sample G2 ($30GeS_2$–$35Sb_2S_3$–35PbS) after annealing at 300°C ($T_g$ + 40°C) for 5 hr, as shown in Fig. 1.2b, while after further annealing for 15 hr, only very weak crystal peaks were observed in its XRD patterns, as shown in Fig. 1.3c.

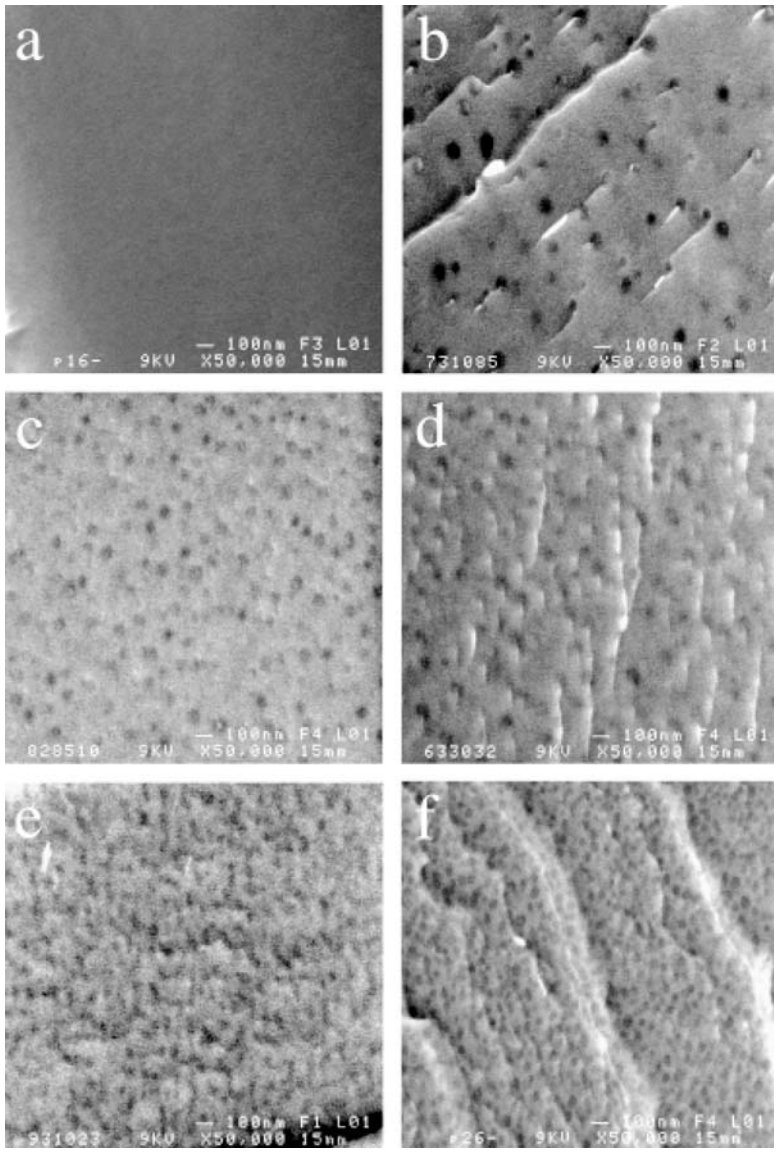


**Figure 1.2** SEM observations after annealing (a) G1 at 330°C for 163 hr, (b) G2 at 300°C for 5 hr, (c) G3 at 340°C for 15 hr, (d) G3 at 310°C for 15 hr, (e) G3 at 310°C for 32 hr, and (f) G3 at 310°C for 85 hr.

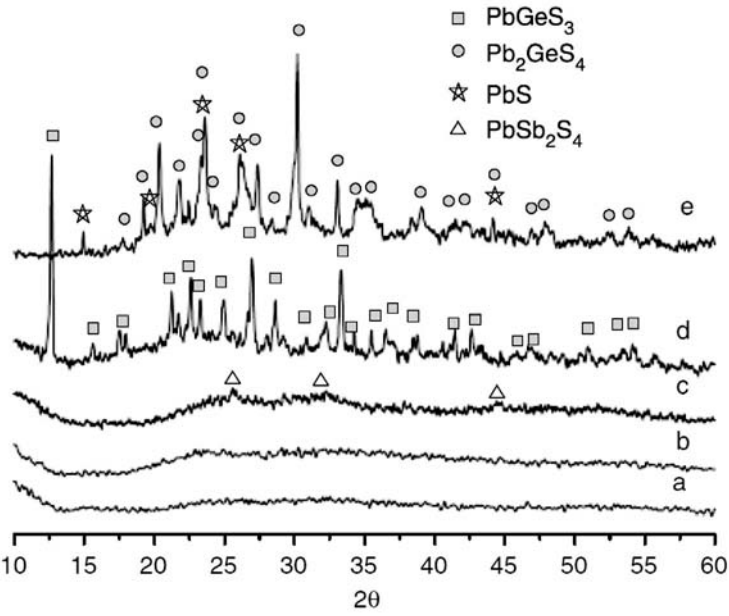


**Figure 1.3** XRD patterns of (a) a G3 glass matrix, (b) G3 after annealing at 340°C for 15 hr, (c) G2 at 300°C for 5 hr, (d) G3 at 310°C for 85 hr, and (e) G4 at 330°C for 12 hr.

Compositions suitable for controlled crystallization treatment fall into the dark shadow area of the glass-forming region (Fig. 1.1), which are classified as substable glasses (SSGs). With these glasses under proper annealing conditions, IR-transmitting glass ceramics with improved physical and thermal properties can be obtained.

Figure 1.4 shows IR transmission spectra of sample G3 ($51GeS_2$–$9Sb_2S_3$–40PbS) before and after annealing under different conditions. It is seen that when annealing it at a higher temperature (340°C, $T_g$ + 45°C) for 15 hr, the electronic absorption cutoff edge moves to a 2 μm wavelength and the glass becomes almost opaque in the wavelength range shorter than 2 μm. This obviously resulted from light scattering on larger-sized crystals, as confirmed by the SEM observation in Fig. 1.2c. At a lower annealing temperature, 310°C ($T_g$ + 15°C), for different durations, however, considerably small-sized (<100 nm) crystals are dispersed homogenously in glass matrices, as shown in Fig. 1.2d–f. Although IR transmission spectra show the

obvious red shift of bandgap that is proportional to the annealing time, it is far from application windows.

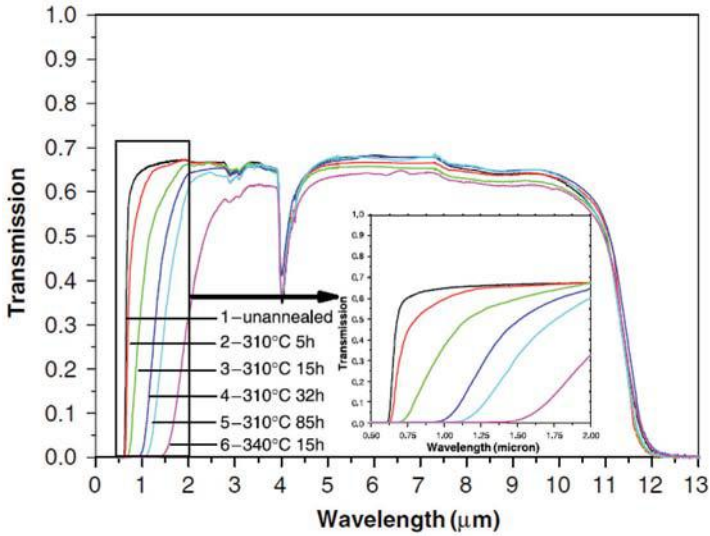


**Figure 1.4** IR transmission spectra of sample G3 before and after annealing under different conditions.

On the other hand, glass ceramics derived from substable compositions possess higher fracture toughness ($K_c$) and lower thermal expansion coefficients ($\alpha$) in comparison with glass matrices. For example, Fig. 1.5 shows that after annealing the glass sample G3 at 310°C for 100 hr, $K_c$ increases from 0.32 MPa·m$^{1/2}$ to 0.49 MPa·m$^{1/2}$ and $\alpha$ decreases from 14.8 × 10$^{-6}$ K$^{-1}$ to 11.7 × 10$^{-6}$ K$^{-1}$. At the same time, the IR transmission of glass ceramics beyond 2 μm is nearly the same as before annealing. Different crystals precipitated from glass matrices are related to glass compositions, as identified by XRD in Fig. 1.3. For example, the main crystals for samples G2, G3, and G4 (42.5$GeS_2$–7.5$Sb_2S_3$–50PbS) are $PbSb_2S_4$, $PbGeS_3$, and $Pb_2GeS_4$, respectively.

## 1.2 The $GeSe_2$–$As_2Se_3$–PbSe System

The glass-forming region in the $GeSe_2$–$As_2Se_3$–PbSe system was determined where the higher lead content could be introduced

in the $As_2Se_3$-rich region than in the $GeSe_2$-rich region. With the introduction of PbSe, the density of glass increases and the calculated molar volume decreases, while the crystallization tendency increases. The activation energy of crystallization and the Avrami exponents are obtained using the modified Ozawa equation. Under proper annealing conditions, suitable IR transmittance glass ceramics are obtained.

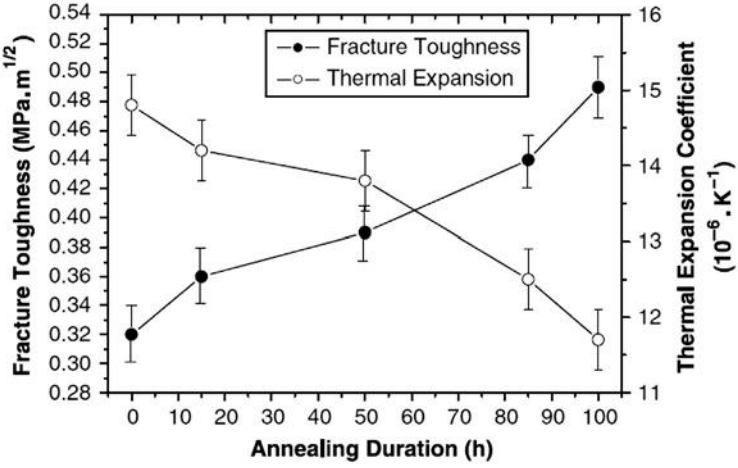


**Figure 1.5** Fracture toughness and thermal expansion coefficient of sample G3 as a function of annealing duration at 310°C. The lines are drawn as a guide to the eye.

### 1.2.1 Glass-Forming Region

The glass-forming region of the $GeSe_2$–$As_2Se_3$–PbSe system is shown in Fig. 1.6 [4]. The system shows fairly good glass-forming ability, with the maximum Pb addition up to 15.15 at.%. Glasses can be obtained along the whole line of $GeSe_2$–$As_2Se_3$ due to the fact that [$GeSe_4$] and [$AsSe_3$] units are good glass formers [5]. Besides, more Pb content can be introduced into the $As_2Se_3$-rich region than in the $GeSe_2$-rich region, indicating that the larger content of $As_2Se_3$ enables a higher involvement of PbSe in the present glass system. Further glasses obtained with the composition along the line of $As_2Se_3$–PbSe can be attributed to the thermodynamic factor.